Article

Novel Sulfone 2-Aminobenzimidazole Derivatives and Their Coordination Compounds: Contribution of the Ethyl and Phenyl Substituents on Non-Covalent Molecular Interactions; Biological Antiproliferative Activity

David Colorado-Solís [1], Rodrigo Castro-Ramírez [1], Francisco Sánchez-Bartéz [2], Isabel Gracia-Mora [2] and Norah Barba-Behrens [1,*]

[1] Departamento de Química Inorgánica, Facultad de Química, Universidad Nacional Autónoma de México, Ciudad Universitaria, Coyoacán, Ciudad de México 04510, Mexico; davidcsolis@hotmail.com (D.C.-S.); rozurigokas@gmail.com (R.C.-R.)

[2] Unidad de Investigación Preclínica (UNIPREC), Facultad de Química, Universidad Nacional Autónoma de México, Ciudad Universitaria, Coyoacán, Ciudad de México 04510, Mexico; francisco.bartez@gmail.com (F.S.-B.); isabel.gracia@gmail.com (I.G.-M.)

[*] Correspondence: norah@unam.mx

Abstract: New sulfone 2-aminobenzimidazole derivatives were designed and synthesized. Their nickel(II), copper(II), zinc(II), cadmium(II) and mercury(II) compounds were obtained and fully characterized by spectroscopic and analytical techniques. Single crystal X-ray structural analysis was performed in order to study the relevant intra and inter non-covalent interactions, mainly H$\cdots\pi$, lone pair$\cdots\pi$, and $\pi\cdots\pi$, highlighting the difference between the terminal ethyl and phenyl groups in such interactions. Dimeric and trimeric supramolecular syntons were found for some of these compounds. Additionally, their antiproliferative activity was investigated, finding that the copper(II) compounds with the sulfone phenyl derivative were the most active.

Keywords: 2-aminobenzimidazole derivatives; ethyl; phenyl substituents; non-covalent interactions H$\cdots\pi$; lone pair$\cdots\pi$; $\pi\cdots\pi$; transition metal complexes; biological activity

1. Introduction

Since the pioneering work of *cis*-platinum and other related platinum compounds [1], biologically active coordination compounds became a new field for bioinorganic chemistry. Platinum is still part of many newly synthetic compounds that attempt to use the covalent mechanism of *cis*-platinum but using different ligands [2,3]. Although *cis*-platinum and other metallic compounds are quite useful and effective, their well-known toxicity [4,5] is still a problem to overcome by the design of new compounds with fewer side effects [6]. There is an interest on focusing on coordination compounds of essential trace elements, such as Fe, Co, Ni, Cu and Zn [7–9], commonly found in biological systems as part of metalloproteins or cofactors for many enzymes [10]. The use of trace elements aims to take advantage of pre-existent metabolic routes, so they could be less toxic than heavier metals.

Considerable research has been undertaken to elucidate the biological activity of coordination compounds and how they work inside human cells. Different mechanisms have been proposed, mainly related to the molecular structure of the compounds, such as redox activity of the ligand or its metal center, covalent bonding to DNA and other biomolecules, non-covalent interactions with biomolecules or a combination of them [11]. While redox activity and covalent bonding are more direct and unspecific, a mechanism based on non-covalent interactions may be more difficult to elucidate, but it will be more sensitive to changes in the structure of the coordination compound and the conformation adopted by the biomolecules [12–14].

DNA is an example of the different ways in which the same biomolecule interacts with transition metal coordination compounds. With B-DNA, the complexes may interact through the phosphate backbone of the strands, stablishing interactions with the nitrogenated bases at the mayor or the minor grooves, intercalation of aromatic moieties between two nucleotides or a combination of these possibilities. All these interactions lead to conformational changes of this biomolecule, affecting its stability and the processes in which it is involved [15]. An example of the relevance of the specificity of non-covalent interactions is found with the interaction of coordination compounds with the quadruplex conformation of DNA, found at the telomeres of chromosomes in guanine rich sections, and that has been related to cell aging and apoptosis [16–20]

The continuous study of non-covalent interactions has been relevant to the design of biologically active compounds [21]. We have been interested in the design of biologically active ligands and their corresponding transition metal coordination compounds, specifically focused on the influence of non-covalent interactions into their biological properties [22].

In previous work with tinidazole (tnz) and its copper(II) and zinc(II) compounds, it was found that tetrahedral coordination compounds showed excellent antiparasitic or antibacterial activity [23,24]. An important factor for the activity of these compounds was the presence of a bifurcated intramolecular lone pair···π interaction (lp), within an O atom of the sulfone group with both imidazolic rings from the coordinated tnz ligands. This interaction stabilized the molecular tetrahedral structure, allowing it to be conserved in solution. The biological activity of the tinidazole copper(II) compounds was further investigated. Different counterions were used to generate tnz-based complexes of various geometries to study the influence of the geometry in the biological activity. Cyclic voltammetry and gel electrophoresis experiments were performed to evaluate their oxidative-damaging properties, and their redox properties were attributable to both the ligand and the metal ion, as has been observed in similar tinidazole compounds [25]. Additionally, DNA-interacting ability and cytotoxicity of tnz copper(II) complexes were evaluated. These complexes interact with DNA by means of electrostatic interactions or/and groove binding. In the presence of a reducing agent, these compounds induce DNA damage by ROS generation. Cytotoxicity studies with different cancer cell lines revealed that complexes $[Cu(tnz)_2(\mu\text{-}Cl)Cl]_2$ and $[Cu(tnz)_2Br_2]$ showed the highest cytotoxicity, while being moderately toxic to normal cells [26,27]

Generally, the reported cytotoxic transition metal compounds have been synthesized using chelating ligands [28–34]. The results with non-chelating ligands, tinidazole and clotrimazole [35–42], have shown that weak interactions, such as hydrogen bonding, electrostatic interactions, π stacking, lp···π or hydrophobic contacts, as well as geometry and redox properties, have an important role in the biological activity of coordination compounds with monocoordinated ligands.

Based on these results, we were interested in investigating 2-aminobenzimidazole sulfonated derivatives, where the presence of the amino group has been found to be of great importance for interactions with biomolecules, thanks to the high hydrogen donor character of the group [12]. These interactions have been observed in previous studies of coordination compounds with the unsubstituted 2-aminobenzimidazole ligand, where the -NH_2 gives place to intramolecular hydrogen bonding with the coordinated halides or acetates stabilized in the molecular structure [43,44]. Additionally, the sulfone group gives place to weak interactions, lp···π contacts and, the presence of a phenyl group, yields π···π stacking interactions [45].

Herein we present the structural and spectroscopic characterization, as well as a non-covalent interactions analysis of the ethyl and phenyl sulfonated ligands, 2-amino-1-(2-phenylsulphonyl)ethylbenzimidazole (*sfabz*); 2-amino-1-(2-ethylsulfonyl) ethylbenzimidazole (*seabz*) and their coordination compounds. The antiproliferative activity of the obtained compounds was also investigated.

2. Results and Discussion

2.1. Spectroscopic Characterization and Magnetic Susceptibility

Chlorido and bromido, Ni^{II}, Cu^{II}, Zn^{II}, Cd^{II} and Hg^{II} coordination compounds of 2-amino-1-(2-phenylsulfonyl)ethylbenzimidazole (*sfabz*) and 2-amino-1-(2-ethylsulfonyl)ethylbenzimidazole (*seabz*), were obtained. Their general structures were proposed based on spectroscopical data as well as elemental analyses. When single crystals were obtained, the proposed structure was confirmed by the X-ray diffraction structure. The magnetic moments were also determined.

2.1.1. IR Spectra

The phenylsulfonated ligand (*sfabz*) presented the $\nu_{as}(NH_2)$ and the $\nu_s(NH_2)$ vibrations in 3434 and 3341 cm^{-1}, respectively; it also presented a band at 1664 cm^{-1} that was assigned as the contributions from the $\nu(C=C)$, the $\delta_{sc}(NH_2)$ and the $\nu(C2-N3)$ vibrations. In a similar way, the band at 1552 cm^{-1} was assigned as the sum of the contributions from the $\nu(C=N)$, the $\rho(NH_2)$ and the $\nu(C2-N10)$ vibrations. Finally, the spectra presented bands at 1286 and 1140 cm^{-1}, which were assigned to the $\nu_{as}(SO_2)$ and $\nu_s(SO_2)$ vibrations, respectively (Figure S1). Benzimidazolic bands were assigned as proposed by Sudha and coworkers [46].

Upon coordination of *sfabz* through the N3, the band centered in 1664 cm^{-1} was shifted to lower energy (1656–1627 cm^{-1}). Additionally, the sulfone bands, $\nu_{as}(SO_2)$ and $\nu_s(SO_2)$, were shifted to higher energy (1294–1289 cm^{-1} and 1144–1141 cm^{-1}, respectively). Only in compounds **5** and **10** was the $\nu_s(SO_2)$ band shifted to lower energy (1138–1136 cm^{-1}). This can be attributable to the different non-covalent interactions this group presented in the different compounds (vide infra).

On the other hand, the ethylsulfonated ligand (*seabz*) presented bands at 3460 and 3373 cm^{-1}, assigned to the $\nu_{as}(NH_2)$ and $\nu_s(NH_2)$ vibrations, respectively. Additionally, the bands at 1639 and 1549 cm^{-1} were assigned in the same composed way as in the *sfabz* ligand (Figure S2). Finally, bands at 1281 and 1132 cm^{-1}, attributed to the $\nu_{as}(SO_2)$ and $\nu_s(SO_2)$ and both vibrations of the amino group (3414–3365 cm^{-1} and 3332–3306 cm^{-1}, respectively), were shifted upon coordination (examples of the IR spectra for coordination compounds with *sfabz* and *seabz* are depicted in Figure S3 and Figure S4, respectively).

2.1.2. Electronic Spectroscopy and Magnetic Susceptibility

For all nickel(II) and copper(II) compounds, the effective magnetic moment was determined and the UV-Vis-NIR was recorded. All the nickel(II) compounds were assigned to a tetrahedral geometry and because of that it was possible to calculate the ν_1 transition according to the graphical method described by Lever [47]. The assigned transitions, as well as the effective magnetic moment are shown in Table 1.

Table 1. Electronic transitions and assignations for the nickel(II) and copper(II) compounds.

Compound	$\nu_1 = {}^3T_2(F) \leftarrow {}^3T_1(F)$	$\nu_2 = {}^3A_2(F) \leftarrow {}^3T_1(F)$	$\nu_3 = {}^3T_1(P) \leftarrow {}^3T_1(F)$	μ_{eff} (B.M.)
[Ni(sfabz)$_2$Cl$_2$] (**1**)	5241 cm^{-1}	9257 cm^{-1}	16,993 cm^{-1}	3.85
[Ni(sfabz)$_2$Br$_2$] (**2**)	5143 cm^{-1}	9778 cm^{-1}	16,135 cm^{-1}	3.91
[Ni(seabz)$_2$Cl$_2$] (**3**)	5423 cm^{-1}	10,250 cm^{-1}	16,690 cm^{-1}	3.60
[Ni(seabz)$_2$Br$_2$] (**4**)	5312 cm^{-1}	10,096 cm^{-1}	16,454 cm^{-1}	3.64
Compound	$\nu_1 = {}^2T \leftarrow {}^2E$ **Solid State**	$\nu_1 = {}^2T \leftarrow {}^2E$ **DMSO Solution**	---	μ_{eff} (B.M.)
[Cu(sfabz)$_2$Cl$_2$] (**5**)	11,000 cm^{-1}	11,049 cm^{-1} (905 nm)	---	1.88
[Cu(sfabz)$_2$Br$_2$] (**6**)	8670 cm^{-1}	11,481 cm^{-1} (871 nm)	---	1.91
[Cu(seabz)$_2$Cl$_2$] (**7**)	9506 cm^{-1}	10,989 cm^{-1} (910 nm)	---	2.15
[Cu(seabz)$_2$Br$_2$] (**8**)	8526 cm^{-1}	11,521 cm^{-1} (868 nm)	---	2.16

The electronic transitions agree with the expected values for a nickel(II) (d^8) tetrahedral compounds. The effective magnetic moment for these complexes is well within the range of 3.2–4.1 B.M. for nickel(II) showing this geometry [48]. Furthermore, the experimental results presented here are supported by their X-ray structure (vide infra).

Similarly, the diffuse reflectance electronic spectra for copper(II) compounds **5–8**, show the d-d transition ca. 10,000 cm^{-1}. Previously reported distorted tetrahedral copper(II) compounds have shown d-d transitions around these values [49,50]. To further assess the stability of these compounds in solution, the spectra in a DMSO solution was obtained. Table 1 shows the values of the d-d electronic transitions at similar values to those in solid state, suggesting the conservation of the ligands in solution (Figures S5 and S6). Compounds **5–8** depict a μ_{eff} within the expected range of 1.8–2.2 B.M. [48].

2.1.3. NMR Studies

^{1}H, ^{13}C and HSQC spectra were obtained for both ligands and compounds **9**, **11**, **13**, **14**, **15** and **16**. The ^{1}H-NMR and ^{13}C-NMR signals were assigned, according to Figure 1a, and are in agreement with the HSQC spectra (Tables S5 and S6). Similarly, Figure 1b, depicts the assignation for the ligand *seafz*, corroborated through HSQC (Tables S7 and S8).
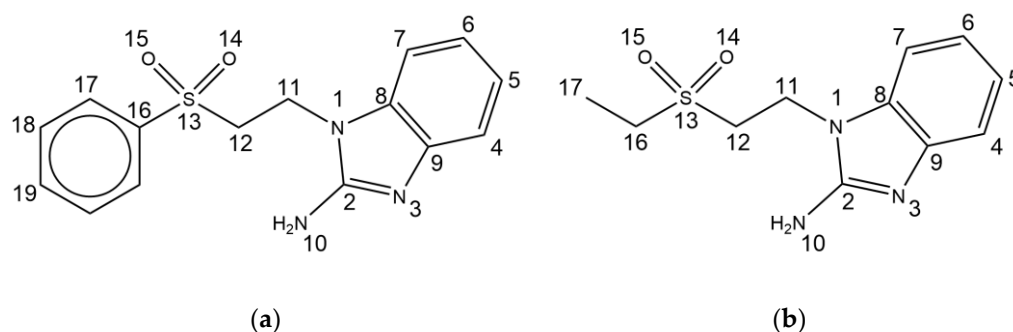

(a)   **(b)**

Figure 1. NMR number assignation for (**a**) *sfabz* and (**b**) *seabz*.

For both series of coordination compounds, signals of the ligands, in both ^{1}H and ^{13}C spectra, are shifted upon coordination ($\Delta\delta$ = ligand-complex, $\Delta\delta > 0.05$ ppm for ^{1}H and $\Delta\delta > 0.1$ ppm for ^{13}C). Tables 2 and 3 resume the effect of coordination in the ^{1}H and ^{13}C signals of the ligands except for their ethyl and phenyl substituents.

Table 2. Values of $\Delta\delta$ for the ^{1}H-NMR data. (N.S. = Not significant).

Position	sfabz Series (Zn/Cd/Hg)		seabz Series (Zn/Cd/Hg)	
	$\Delta\delta$ (ppm)	Effect	$\Delta\delta$ (ppm)	Effect
H4	0.16/0.17/0.17	deshielding	0.13/0.21/0.17	deshielding
H5	0.05/N.S./0.09	deshielding	0.11/0.10/0.14	deshielding
H6	0.13/0.06/0.15	deshielding	0.08/N.S./0.09	deshielding
H7	0.18/0.08/0.20	deshielding	0.13/0.08/0.14	deshielding
H10	0.78/0.32/0.69	deshielding	0.84/0.38/0.65	deshielding
H11	0.12/N.S./0.11	deshielding	0.11/N.S./0.08	deshielding
H12	0.09/N.S./0.09	deshielding	0.09/N.S./0.06	deshielding

According to the ^{1}H spectra, it is possible to differentiate the behavior of the three groups of protons: the benzimidazolic protons, the amino group, and the aliphatic chain protons. For the benzimidazolic protons of both series of compounds, the deshielding effect is more pronounced in H6 and H7 and smaller in H5. Comparing the effect of different metals, the deshielding at H5-H7 follows the trend Hg = Zn < Cd, while at H4 all metals cause almost similar displacements in the *sfabz* series and Cd causes the bigger effect in the *seabz* series.

In both ligands' series the amino protons are deshielded upon coordination to the metal ion. This effect is more predominant with Zn, and lower with Cd. Similarly, the aliphatic chain shows a significant displacement, with same tendency seen in the amino group, namely, Zn > Hg > Cd.

Table 3. Values of $\Delta\delta$ for the ^{13}C-NMR data.

Position	*sfabz* Series (Zn/Cd/Hg)		*seabz* Series (Zn/Cd/Hg)	
	$\Delta\delta$ (ppm)	Effect	$\Delta\delta$ (ppm)	Effect
C2	0.1/0.2/0.2	deshielding	0.1/0.1/0.2	deshielding
C4	0.7/0.2/0.9	Zn, Hg deshielding Cd shielding	0.8/0.2/0.8	Zn, Hg deshielding Cd shielding
C5	1.1/0.4/1.1	deshielding	1.2/0.5/1.0	deshielding
C6	2.0/1.0/1.9	deshielding	2.0/1.1/1.8	deshielding
C7	1.3/0.5/1.4	deshielding	1.2/0.6/1.1	deshielding
C8	1.6/0.8/1.4	shielding	1.6/0.9/1.3	shielding
C9	3.9/2.0/3.7	shielding	4.4/2.5/3.4	shielding
C11	0.3/0.1/0.5	deshielding	0.2/0.1/0.3	deshielding
C12	0.6/0.3/0.7	shielding	0.6/0.3/0.5	shielding

Comparing the effect of the metal in the ^{13}C spectra, the shielding and deshielding are more pronounced in the Zn compounds and less prominent in the Hg and Cd compounds. The ^{13}C chemical shifts of the aliphatic chain showed a slight deshielding at C11, and a shielding effect on the C12, an effect that can be attributed to the sulfone group in the chain. The terminal chain is also affected by the sulfone, where the aliphatic ethyl chain shows no significant changes in its chemical shifts for both ^{1}H and ^{13}C data, while the phenyl group shows significant changes at the C16 and C17 positions ($\Delta\delta$ C16$_{\text{máx}}$ = 0.5 ppm, $\Delta\delta$ C17$_{\text{máx}}$ = 0.3 ppm).

2.2. X-ray Structures of the Ligands and Their Coordination Compounds

2.2.1. Crystal Structure of the 2-Aminobenzimidazolic Ligands

Despite the difference in the terminal substituent, both the *seabz* and *sfabz* ligands crystallize in a P 2$_1$/n space group, within a monoclinic crystal system. However, these two ligands show different intramolecular interactions. For the *seabz* ligand, one of the oxygen atoms in the sulfone group is orientated towards the benzimidazolic ring, due to a lone pair$\cdots\pi_{\text{bz}}$ interaction at 3.775 Å (Figure 2a), as has been observed in purine nucleobases, where the lone pair$\cdots\pi$ interactions are evenly distributed in the intersection of the fused aromatic rings, [51,52].

Alternatively, the *sfabz* ligand depicts the sulfone group away from the benzimidazolic ring, thus, generating a weak H$\cdots\pi_{\text{phe}}$ at 3.791 Å, between a benzimidazolic proton and the centroid in the terminal phenyl ring (Figure 2b).

Another difference found in the crystal structures of both ligands is the type of intermolecular interactions, mainly the hydrogen bonding involving the N3 of the benzimidazolic ring. The *sfabz* ligand depicts two strong hydrogen bonds with the amino group acting as the donor and the N3, the acceptor. This interaction is at 2.041 Å with an angle of 174.58°. Two neighboring molecules show one of these hydrogen bonds each, forming a dimer as depicted in Figure 3a. On the other hand, the *seabz* ligand also shows a hydrogen bond with the N3 as the acceptor. However, this is a weak hydrogen bond, given the donor is a –CH$_2$– group at 2.603 Å and 157.15°. Alternatively, what seems to be a major stabilizing interaction, between four *seabz* molecules, is a series of hydrogen bonds with the amino group acting as the donor, with the S=O accepting two protons form different molecules. Their angles and distances (2.088 Å, 2.127 Å and 171.03°, 164.33°) indicate that these interactions are moderate. Figure 3b depicts these hydrogen bonds.
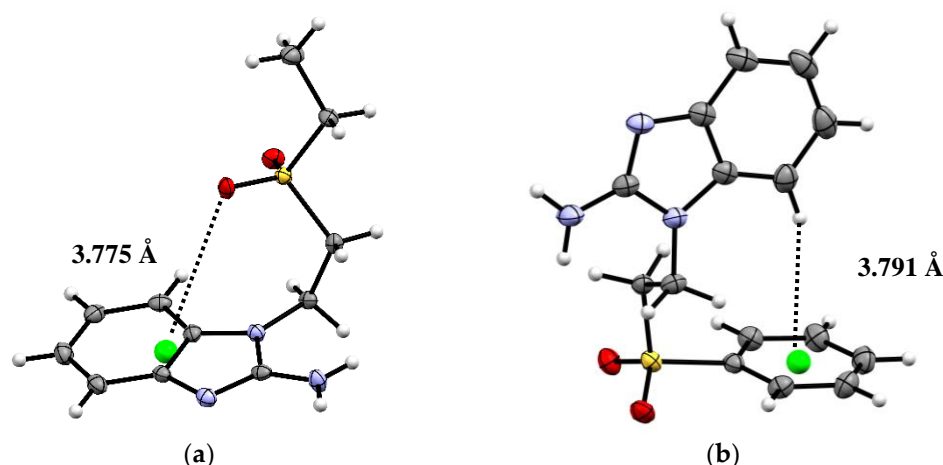
Figure 2. Crystal structure and intramolecular interactions of (**a**) *seabz* with a lp···π_{bz} (green) and (**b**) *sfabz* with a H···π_{phe} (green), ORTEP ellipsoids at 50% probability.

Figure 3. Intermolecular hydrogen bonds forming (**a**) a *sfabz* dimer and (**b**) a *seabz* tetramer.

2.2.2. Crystal Structure of the Coordination Compounds of *seabz* and *sfabz*

Tetrahedral coordination compounds have been synthesized herein with both alkyl-sulfonated benzimidazole ligands to be able to compare the effect of the substituents in the non-covalent interactions found in the crystal structures. As mentioned above, all compounds show the formula [ML$_2$X$_2$] (M^{2+} = Ni, Cu, Zn, Cd, Hg; L = *seabz*, *sfabz*; X = Cl$^-$, Br$^-$), without the presence of water molecules, despite that hydrated metal salts were used to synthesize them. For some of the *seabz* complexes, adequate crystals for X-ray diffraction were not obtained. This could be due to the fact that the ethyl group presents far fewer non-covalent interactions than the phenyl ring does (vide infra). Due to this, for compounds **11**, **14**, and **16**, only basic structural features and connectivity are discussed.

Compounds **1**, **2** (L = *sfabz*) and **3** (L = *seabz*) depict a Ni center with either a Cl$^-$ or Br$^-$ anion. Compounds **1** and **2** are both obtained in a P-1 space group, within a triclinic crystal system, regardless of the acetone molecule from the solvent in compound **2**. Alternatively, compound **3** is obtained in a P 2$_1$/c space group and a monoclinic system. The bond lengths and angles around the metal ion for these three compounds are shown in Table 4. From the results shown in this table, it is noticeable that the terminal substituent in the alkylsulfonated chain does not have a major effect in the bonds around the metal ion.

However, the terminal group affects the interactions that each of these compounds present. Even between the two *sfabz* Ni coordination compounds, different intramolecular contacts are found. The crystal structure for compound **1** (Figure 4a) depicts both ligands in different conformations, one being extended and the other one with both aromatic rings facing each other. In doing so, a H···π_{bz} contact can be found at 2.954 Å. In contrast with the H···π_{phe} interaction observed in the free ligand (vide supra), in the nickel compound this interaction is between two different ligands, where the aromatic rings, acting as donor and acceptor, are reversed giving a H···π_{bz} contact. Compound **2**, also a *sfabz* derivative, shows

a similar interaction, between benzimidazolic moieties. The H··· π_{bz} contact (3.577 Å) is shown in Figure 4b. Finally, compound **3**, rather than depicting a H···π contact, depicts a lone pair···π intramolecular interaction between the sulfone group and the benzimidazolic ring (Figure 4c). This interaction is at 3.416 Å and with an angle *centroid-N-O* of 85.51°, indicative of a strong non-covalent interaction that stabilizes the crystal structure. This emphasizes the importance of the terminal substituent in this type of ligands, when the substituent is a phenyl ring, primarily depicting H···π contacts. Whereas, when it is an ethyl group, this interaction is no longer present, giving place to a different interaction, namely, lp···π.

Table 4. Angles and distances around the metal ion for compounds **1**, **2** and **3**.

Compound	Angle	Degrees (°)	Bond	Distance (Å)
[Ni(sfabz)₂Cl₂] (1)	N-Ni-N′	102.0(1)	Ni-Cl	2.233(9)
	N-Ni-Cl	107.91(9)	Ni-Cl′	2.258(1)
	N-Ni-Cl′	106.21(9)	Ni-N	1.987(3)
	N′-Ni-Cl	111.73(9)	Ni-N′	1.979(3)
	N′-Ni-Cl′	106.22(9)		
	Cl-Ni-Cl′	121.06(3)		
[Ni(sfabz)₂Br₂] (2)	N-Ni-N′	107.94(8)	Ni-Br	2.392(4)
	N-Ni-Br	109.49(6)	Ni-Br′	2.414(4)
	N-Ni-Br′	103.65(6)	Ni-N	1.975(2)
	N′-Ni-Br	112.06(6)	Ni-N′	1.969(2)
	N′-Ni-Br′	109.12(6)		
	Br-Ni-Br′	114.09(2)		
[Ni(seabz)₂Cl₂] (3)	N-Ni-N′	102.00(1)	Ni-Cl	2.256(10)
	N-Ni-Cl	109.09(8)	Ni-Cl′	2.282(9)
	N-Ni-Cl′	108.79(8)	Ni-N	1.967(2)
	N′-Ni-Cl	107.95(8)	Ni-N′	1.974(3)
	N′-Ni-Cl′	107.22(8)		
	Cl-Ni-Cl′	120.25(3)		

Regarding the intermolecular interactions of these nickel(II) complexes, both *sfabz* compounds show very different contacts in their crystal structure. Compound **2** depicts a displaced π···π stacking interaction between two benzimidazolic rings at 3.673 Å (centroid-centroid) (Figure 5b). Alternatively, compound **1** shows hydrogen bonds with the amino and a –CH₂– group acting as the donor, and an oxygen of the sulfone group as the acceptor (Figure 5a). These differences in intermolecular interactions between these two compounds can be attributed, mainly, to the fact that compound **2** crystalizes with an acetone molecule. Performing a similar analysis with compound **3** with *seabz*, what seems to be the most important contact is a lone pair···π interaction between S=O and the benzimidazolic ring at 3.347Å and 89.59°, directed towards the center of the imidazolic ring of this molecule (Figure 5c). Interestingly, the other oxygen of the same sulfone group is the one showing the intramolecular lone pair···π interaction (vide supra). This is relevant because in our previous work with alkylsulfonated ligands [44,45], when one oxygen of the sulfone group is depicting such interactions, the other oxygen does not show any other contact, not even weak hydrogen bonds.

As mentioned above, adequate crystals for X-ray diffraction were easier to obtain with the *sfabz* ligand. However, the copper(II) complex (compound **5**) shows great disorder in one of the *sfabz* ligands. Regardless, it is still possible to see its connectivity and geometrical features. Compound **5** crystalizes in a P-1 space group, within a triclinic system. Although this compound still stabilizes a tetrahedral geometry, it is more distorted than the nickel

and zinc coordination compounds, as its noticeable for its larger N-Cu-N' angle of 135.54°
(Figure 6). No relevant intramolecular contacts could be assigned in this structure, due to
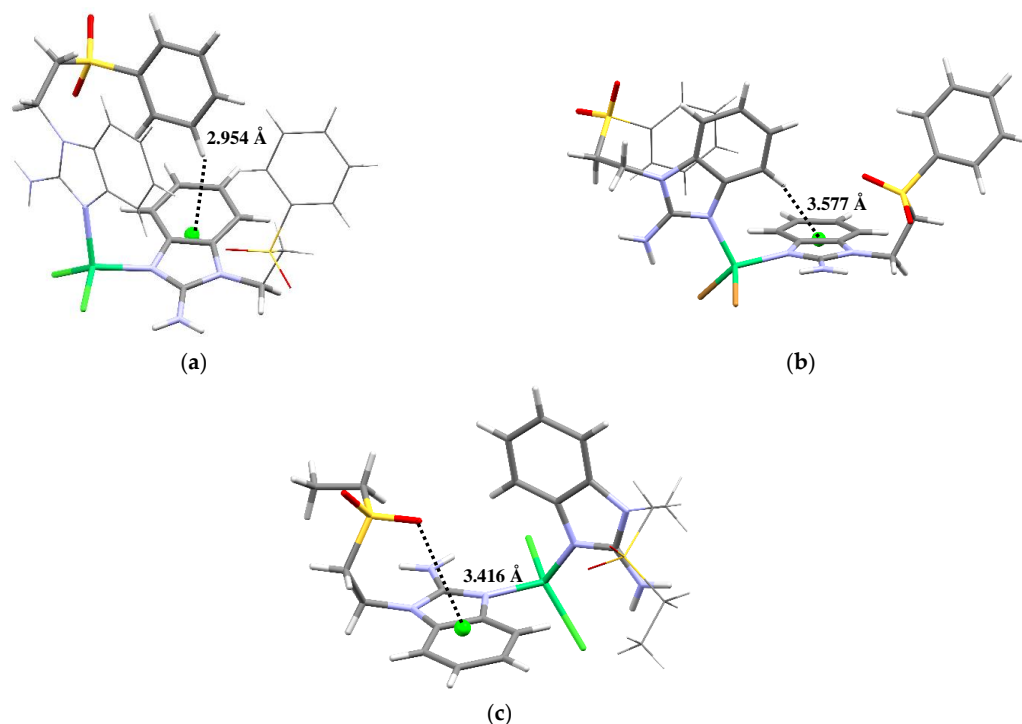the structural disorder.

Figure 4. Intramolecular interactions for (**a**) [Ni(sfabz)$_2$Cl$_2$], depicting a H···π_{bz}, (**b**) [Ni(sfabz)$_2$Br$_2$],
depicting a H···π_{bz} and (**c**) [Ni(seabz)$_2$Cl$_2$], depicting a lp···π_{bz}.
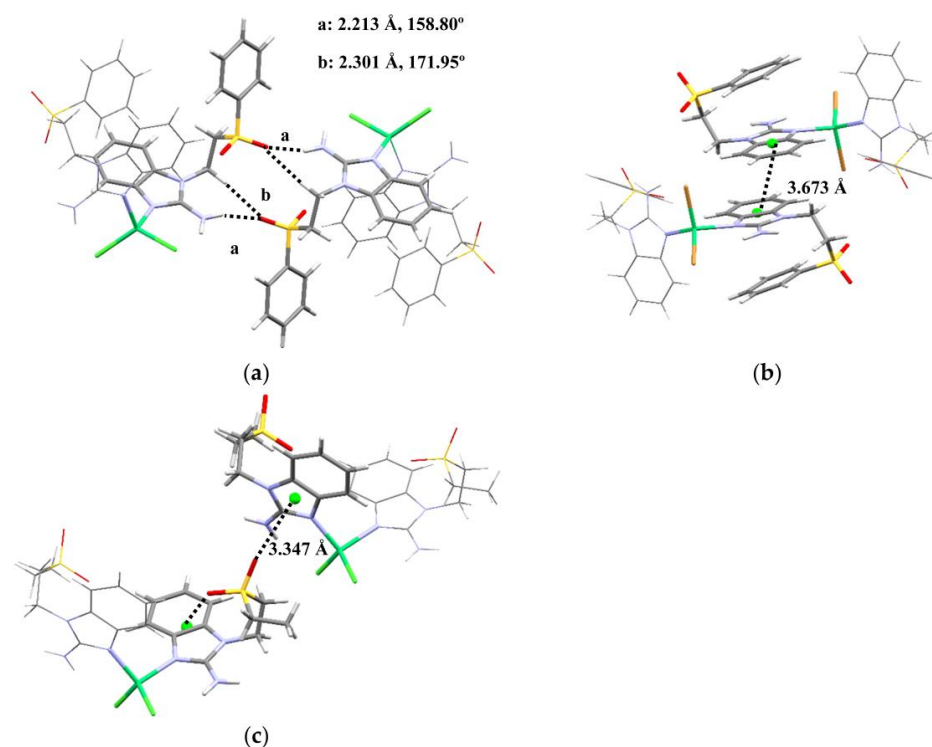
Figure 5. Intermolecular interactions for [Ni(sfabz)$_2$Cl$_2$], (**a**) depicting a hydrogen bonding,
(**b**) [Ni(sfabz)$_2$Br$_2$], depicting π stacking and (**c**) [Ni(seabz)$_2$Cl$_2$], depicting both intra and inter
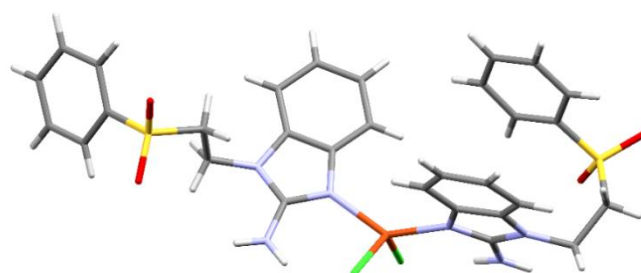lp···π_{bz}.

Figure 6. Crystal structure for compound [Cu(sfabz)$_2$Cl$_2$].

Two compounds with Zn(II) and *sfabz* were obtained, crystallizing in a triclinic system and a P-1 space group. Angles and bond distance around the metal ion are summarized in Table 5. Although compound **10** depicts an acetone molecule in the crystal structure, this does not seem to affect the intramolecular interactions, as both Zn(II) sfabz complexes depict a H⋯π contact with one benzimidazolic ring acting as the donor, and the other one as the acceptor, with a distance of 3.404 Å for compound **9** and 3.630 Å for compound **10**. In contrast with the NiX$_2$ derivatives discussed above, where the crystal structure is either stabilized through either hydrogen bonds with the sulfone or through π stacking between the benzimidazolic rings, compounds **9** and **10** depict both interactions at the same time with one neighboring molecule. Figure 7 shows the intermolecular interactions for compound **9**, as an example with the relevant angle and distances. The corresponding values for compound **10** can be found in parenthesis in the same figure.

Table 5. Angles and distances around the metal ion for compounds **9** and **10**.

Compound	Angle	Degrees (°)	Bond	Distance (Å)
[Zn(sfabz)$_2$Cl$_2$] (9)	N-Zn-N′	108.78(1)	Zn-Cl	2.244(2)
	N-Zn-Cl	106.71(1)	Zn-Cl′	2.285(2)
	N-Zn-Cl′	111.63(1)	Zn-N	1.996(3)
	N′-Zn-Cl	115.17(1)	Zn-N′	1.989(4)
	N′-Zn-Cl′	106.72(1)		
	Cl-Zn-Cl′	107.91(5)		
[Zn(sfabz)$_2$Br$_2$] (10)	N-Zn-N′	111.07(1)	Zn-Br	2.399(6)
	N-Zn-Br	110.34(9)	Zn-Br′	2.430(6)
	N-Zn-Br′	106.04(9)	Zn-N	1.999(3)
	N′-Zn-Br	110.89(9)	Zn-N′	1.992(3)
	N′-Zn-Br′	109.85(9)		
	Br-Zn-Br′	108.52(2)		

a: 2.353 Å, 150.37° (2.172 Å, 148.19°)

b: 2.434 Å, 172.08° (2.699 Å, 168.87°)

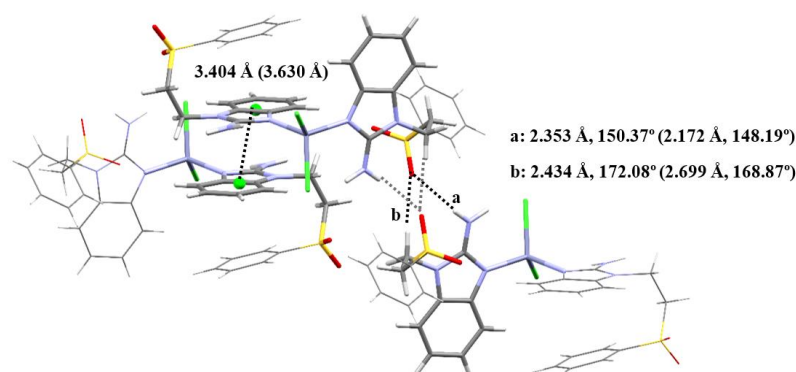**Figure 7.** Intermolecular interactions between three neighboring molecules of [Zn(sfabz)$_2$Cl$_2$].

The connectivity and general structure features for compounds **11**, **14** and **16** (Zn, Cd and Hg, respectively) are depicted in Figure 8. As the obtained crystals were not adequate to properly obtain their X-ray structure, only general aspects of the compounds can be assessed. Namely, all three compounds depict two alkylsulfone ligands and two halogens, yielding tetracoordinated compounds, a distorted tetrahedral geometry, as seen for all the crystal structures depicted herein. It is noteworthy that, for these three compounds, an acetonitrile molecule is present in the crystal structure. This highlights the importance of the solvent being used for crystallization as, even though some crystal structures depict acetone molecules, this does not affect the quality of the X-ray diffractions obtained. Whereas, using acetonitrile as a solvent introduces disorder, and lower-quality crystals are obtained.
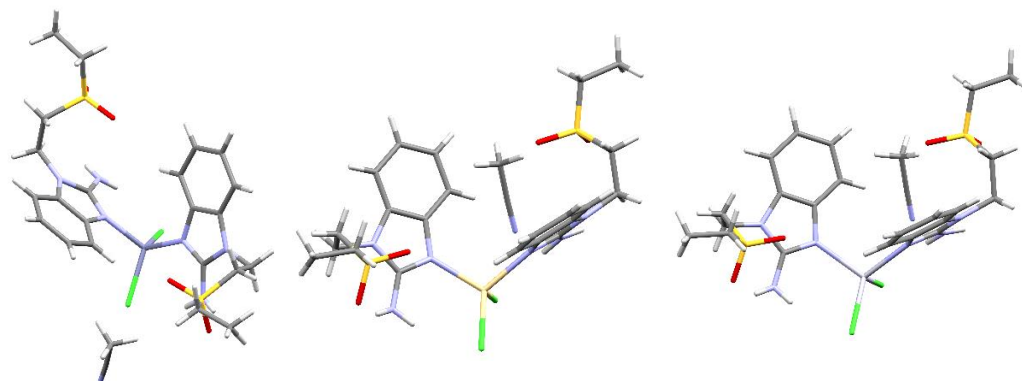

Figure 8. Structural connectivity for compounds left to right: [Zn(seabz)$_2$Cl$_2$], [Cd(seabz)$_2$Cl$_2$] and [Hg(seabz)$_2$Cl$_2$].

2.3. Stability in Solution and Antiproliferative Activity

The stability in solution of the copper(II) compounds was assessed as described in the methods section of this article. In all cases, the same electronic transitions described above were observed without significant change after a day in solution, indicating no changes in the geometry or coordination. As the Cu(II) compounds and zinc(II) compounds showed no significant variation in their NMR spectra after the same time period, both series of compounds are considered as suitable for biological activity studies.

To determine their antiproliferative activity, a cell-viability assay was carried out with the aforementioned copper(II) and zinc(II) compounds against HeLa (cervix carcinoma), HCT-15 (colorectal adenocarcinoma), MCF-7 (breast adenocarcinoma), A549 (lung adenocarcinoma) and L929 (healthy connective mice tissue).

The IC$_{50}$ of the compounds was determined and is presented below (Table 6). As observed in the table, IC$_{50}$ for both ligands was the highest of all compounds for every cancer cell line, indicating that the ligands alone were not active. In fact, most of the coordination compounds were significantly less active than *cis*-platinum in most cancer cell lines. Only copper(II) *sfabz* coordination compounds were active enough to be compared with *cis*-platinum when tested in the HeLa cell line, being [Cu(sfabz)$_2$Br$_2$] (**6**) slightly better than the Pt reference compound.

Although only few compounds showed IC$_{50}$ comparable to cisplatin, there is a visible pattern for the antiproliferative activity of the compounds. Despite the substituent of the benzimidazolic ligand, copper(II) compounds showed higher activity than their zinc(II) homologues. Additionally, bromo-containing compounds were typically more active than their chloro counterparts. Comparing both series of complexes, *seabz* compounds were substantially less active than the *sfabz* compounds.

Finally, all compounds were generally less active than *cis*-platinum towards healthy mice tissue. Given the selectivity of copper(II) *sfabz* compounds on cancer cell lines, they are worth further investigation.

Table 6. IC$_{50}$ values of the copper(II) and zinc(II) compounds for all cell lines.

	HCT-15 IC50 (µM)	MCF-7 IC50 (µM)	HeLa IC50 (µM)	A549 IC50 (µM)	L929 IC50 (µM)
Sfabz	395.4	406.4	386.3	360.4	352.5
[Cu(sfabz)$_2$Cl$_2$] (**5**)	161.3	136.6	29.8	153.6	148.3
[Cu(sfabz)$_2$Br$_2$] (**6**)	133.9	118.6	15.0	135.5	122.5
[Zn(sfabz)$_2$Cl$_2$] (**9**)	140.1	148.5	144.7	170.8	140.9
[Zn(sfabz)$_2$Br$_2$] (**10**)	144.8	130.2	189.8	140.6	137.4
Seabz	898.6	496.7	748.0	1311.8	2364.9
[Cu(seabz)$_2$Cl$_2$] (**7**)	168.8	147.3	109.7	166.9	176.7
[Cu(seabz)$_2$Br$_2$] (**8**)	159.9	139.1	142.0	163.0	147.2
[Zn(seabz)$_2$Cl$_2$] (**11**)	184.2	163.6	194.0	176.9	166.3
[Zn(seabz)$_2$Br$_2$] (**12**)	167.8	160.8	167.3	266.3	150.8
cisplatin	32.7	32.3	19.0	34.9	43.2

3. Experimental

3.1. Materials

2-aminobenzimidazole, phenylvinyl sulfone and ethylvinyl sulfone were purchased from Sigma-Aldrich and used without further purification. The metal salts K$_2$CO$_3$ (99%), CuCl$_2$·2H$_2$O (97%), CuBr$_2$ (98%), NiCl$_2$·6H$_2$O (99%), ZnBr$_2$ (>97%), HgCl$_2$ (98%) and CdCl$_2$·2.5H$_2$O (99%) were purchased from J.T. Baker, the salt ZnCl$_2$ (>97%) was obtained from Sigma Aldrich and the salt NiBr$_2$·3H$_2$O (99%) was purchased from Merck. All solvents were obtained from J.T. Baker. Both salts and solvents were used without further purification.

3.2. Synthesis of the Ligands

3.2.1. Synthesis of 2-Amino-1-(2-phenylsulfonyl)ethylbenzimidazole (sfabz)

The ligand was synthesized by mixing phenylvinyl sulfone (3.3182 mmol, 0.5582 g), 2-aminobenzimidazole (3.3182 mmol, 0.4418 g), and K$_2$CO$_3$ (1.6591 mmol, 0.2293 g) in 10 mL of acetonitrile. The mixture was stirred under reflux for ten minutes, left to stand at room temperature and then filtered. The precipitate was washed with a concentrated solution of NH$_4$Cl and then with distilled water. Crystals suitable for single crystal X-ray diffraction were obtained by slow evaporation of a solution of the ligand in methanol. Yield: 92%. Anal. calculated for C$_{15}$H$_{15}$N$_3$O$_2$S: C, 59.78%; H, 5.02%; N, 13.95%; S, 10.62%. Experimental: C, 59.58%; H, 4.82%; N, 14.19%; S, 10.76%. IR (ν cm^{-1}): vs. 3434 ν_{as}(NH$_2$), w 3341 ν_s(NH$_2$), vs. 1664 ν(C=C) + δ_{sc}(NH$_2$) + ν(C2-N3), vs. 1552 ν(C=N) + ρ(NH$_2$) + ν(C2-N10), s 1286 ν_{as}(SO$_2$), s 1140 ν_s(SO$_2$). RMN: δ 7.86 (H17, d, J = 7.4 Hz, 2H), 7.71 (H19, t, J = 7.4 Hz, 1H), 7.58 (H18, t, J = 7.4 Hz, 2H), 7.05 (H4, d, J = 7.5 Hz, 1H), 6.89 (H5, t, J = 7.5, 1H), 6.79 (H6, t, J = 7.5 Hz, 1H), 6.74 (H7, d, J = 7.5 Hz, 1H), 6.43 (H10, s, 2H), 4.28 (H11, t, J = 7.0 Hz, 2H), 3.72 (H12, t, J = 7.0 Hz, 2H).

3.2.2. Synthesis of 2-Amino-1-(2-ethylsulfonyl)ethylbenzimidazole (seabz)

The ligand was prepared by mixing ethylvinyl sulfone (4.768 mmol, 0.5755 g) and 2-aminobenzimidazole (4.768 mmol, 0.6376 g) in 10 mL of acetonitrile. This mixture was stirred under reflux for 30 min, then was left to stand at room temperature. The precipitate was filtered and washed with 5 mL of ethylacetate. Crystals suitable for single crystal X-ray diffraction were obtained by slow evaporation of a solution of the ligand in methanol. Yield: 66%. Anal. calculated for C$_{11}$H$_{15}$N$_3$O$_2$S: C, 51.24%; H, 6.06%; N, 16.30%; S, 12.44%. Experimental: C, 51.27%; H, 5.93%; N, 16.35%; S, 12.50%. IR (ν cm^{-1}): vs. 3460 ν_{as}(NH$_2$), vs. 3373 ν_s(NH$_2$), vs. 1639 ν(C=C) + δ_{sc}(NH$_2$) + ν(C2-N3), vs. 1549 ν(C=N) + ρ(NH$_2$) + ν(C2-N10), s 1281 ν_{as}(SO$_2$), s 1132 ν_s(SO$_2$). RMN: δ 7.13 y 7.15 (H4 y H7, dd, J = 7.4, 1.2 Hz, 2H), 6.94 (H6, td, J = 7.4, 1.2 Hz, 1H), 6.88 (H5, td, J = 7.4, 1.2 Hz, 2H), 6.48 (H10, s, 2H), 4.39 (H11,

d, J = 7.2 Hz, 2H), 3.46 (H12, t, J = 7.2 Hz, 2H), 3.08 (H16, q, J = 7.4 Hz, 2H), 1.15 (H17, t, J = 7.4 Hz, 2H).

3.3. Synthesis of the Coordination Compounds

Coordination compounds of *sfabz* and *seabz* were synthesized by similar procedures. A mixture of the ligand and the metal salt in a methanol solution (10 mL) was stirred under reflux for 30 min. The reaction mixture was left to stand at room temperature, the obtained products were filtered and washed with cold ethanol. Details of the reaction conditions are discussed below.

3.3.1. [Ni(sfabz)$_2$Cl$_2$] (**1**)

A solution of the ligand (0.1507 g, 0.5 mmol) and NiCl$_2 \cdot$6H$_2$O (0.0594 g, 0.25 mmol) in 15 mL of ethanol was stirred under reflux for 30 min. The reaction mixture was left to stand at room temperature. The obtained product was filtered and washed with 10 mL of cold ethanol. Crystals suitable for single crystal X-ray diffraction were obtained preparing a solution in acetone of the solid obtained and leaving it to slow evaporation. Yield: 80%. Anal. calculated for NiC$_{30}$H$_{32}$N$_6$O$_5$S$_2$Cl$_2$: C, 48.02%; H, 4.30%; N, 11.20%; S, 8.55%. Experimental: C, 47.62%; H, 3.56%; N, 10.80%; S, 8.01%. IR (ν cm^{-1}): s 3387 ν_{as}(NH$_2$), s 3305 ν_s(NH$_2$), vs. 1645 ν(C=C) + δ_{sc}(NH$_2$) + ν(C2-N3), vs. 1552 ν(C=N) + ρ(NH$_2$) + ν(C2-N10), s 1292 ν_{as}(SO$_2$), s 1141 ν_s(SO$_2$).

3.3.2. [Ni(sfabz)$_2$Br$_2$] (**2**)

A solution of the ligand (0.1507 g, 0.5 mmol) and NiBr$_2 \cdot$3H$_2$O (0.0681 g, 0.25 mmol) in 15 mL of ethanol was stirred under reflux for 30 min. The reaction mixture was left to stand at room temperature. The obtained product was filtered and washed with 10 mL of cold ethanol. The compound was dissolved in acetone, and crystals suitable for single crystal X-ray diffraction were obtained by slow evaporation of the solvent. Yield: 71%. Anal. calculated for NiC$_{30}$H$_{30}$N$_6$O$_4$S$_2$Br$_2$: C, 43.88%; H, 3.68%; N, 10.23%; S, 7.81%. Experimental: C, 43.56%; H, 3.20%; N, 10.10%; S, 7.66%. IR (ν cm^{-1}): s 3418 ν_{as}(NH$_2$), s 3307 ν_s(NH$_2$), s 1643 ν(C=C) + δ_{sc}(NH$_2$) + ν(C2-N3), vs. 1549 ν(C=N) + ρ(NH$_2$) + ν(C2-N10), vs. 1290 ν_{as}(SO$_2$), vs. 1146 ν_s(SO$_2$).

3.3.3. [Ni(seabz)$_2$Cl$_2$] (**3**)

A solution of the ligand (0.1267 g, 0.5 mmol) and NiCl$_2 \cdot$6H$_2$O (0.0594 g, 0.25 mmol) in 15 mL of ethanol was stirred under reflux for 30 min. The reaction mixture was left to stand at room temperature. The obtained product was filtered and washed with 10 mL of cold ethanol. The compound was dissolved in acetone, and crystals suitable for single crystal X-ray diffraction were obtained by slow evaporation of the solvent. Yield: 89%. Anal. calculated for NiC$_{22}$H$_{34}$N$_6$O$_6$S$_2$Cl$_2$: C, 39.31%; H, 5.10%; N, 12.50%; S, 9.54%. Experimental: C, 39.69%; H, 4.82%; N, 12.56%; S, 8.80%. IR (ν cm^{-1}): m 3407 ν_{as}(NH$_2$), s 3321 ν_s(NH$_2$), vs. 1646 ν(C=C) + δ_{sc}(NH$_2$) + ν(C2-N3), s 1559 ν(C=N) + ρ(NH$_2$) + ν(C2-N10), s 1295 ν_{as}(SO$_2$), s 1128 ν_s(SO$_2$).

3.3.4. [Ni(seabz)$_2$Br$_2$] (**4**)

A solution of the ligand (0.1267 g, 0.5 mmol) and NiBr$_2 \cdot$3H$_2$O (0.0681 g, 0.25 mmol) in 15 mL of ethanol was stirred under reflux for 30 min. The reaction mixture was left to stand at room temperature. The obtained product was filtered and washed with 10 mL of cold ethanol. Yield: 69%. Anal. calculated for NiC$_{22}$H$_{35}$N$_6$O$_{6.5}$S$_2$Br$_2$: C, 34.31%; H, 4.58%; N, 10.91%; S, 8.37%. Experimental: C, 33.97%; H, 4.11%; N, 11.25%; S, 7.84%. IR (ν cm^{-1}): vs. 3387 ν_{as}(NH$_2$), vs. 3311 ν_s(NH$_2$), vs. 1645 ν(C=C) + δ_{sc}(NH$_2$) + ν(C2-N3), vs. 1550 ν(C=N) + ρ(NH$_2$) + ν(C2-N10), vs. 1294 ν_{as}(SO$_2$), s 1126 ν_s(SO$_2$).

3.3.5. [Cu(sfabz)₂Cl₂] (**5**)

A solution of 0.0426 g (2.5 mmol) of CuCl₂·2H₂O and 0.2260 g (7.5 mmol) of the ligand *sfabz* in 15 mL of ethanol was stirred under reflux for one hour. The reaction mixture was left to stand at room temperature. The obtained product was filtered and washed with 10 mL of cold ethanol. Crystals suitable for single crystal X-ray diffraction were obtained by slow evaporation of the remanent ethanolic reaction mixture. Yield: 65%. Anal. calculated for $CuC_{30}H_{31}N_6O_{4.5}S_2Cl_2$: C, 48.29%; H, 4.19%; N, 11.26%; S, 8.60%. Experimental: C, 48.10%; H, 3.94%; N, 11.36%; S, 8.95%. IR (ν cm^{-1}): m 3440 ν_{as}(NH₂), m 3372 ν_s(NH₂), s 1638 ν(C=C) + δ_{sc}(NH₂) + ν(C2-N3), m 1546 ν(C=N) + ρ(NH₂) + ν(C2-N10), s 1289 ν_{as}(SO₂), s 1138 ν_s(SO₂).

3.3.6. [Cu(sfabz)₂Br₂] (**6**)

A solution of the ligand (0.1507 g, 0.5 mmol) and CuBr₂ (0.0558 g, 0.25 mmol) in 15 mL of ethanol was stirred under reflux for 30 min. The reaction mixture was left to stand at room temperature. The obtained product was filtered and washed with 10 mL of cold ethanol. Yield: 97%. Anal. calculated for $CuC_{30}H_{32}N_6O_5S_2Br_2$: C, 42.69%; H, 3.82%; N, 9.96%; S, 7.60%. Experimental: C, 42.41%; H, 3.49%; N, 9.87%; S, 7.31%. IR (ν cm^{-1}): m 3525 ν_{as}(NH₂), s 3318 ν_s(NH₂), s 1643 ν(C=C) + δ_{sc}(NH₂) + ν(C2-N3), m 1557 ν(C=N) + ρ(NH₂) + ν(C2-N10), s 1294 ν_{as}(SO₂), vs. 1141 ν_s(SO₂).

3.3.7. [Cu(seabz)₂Cl₂] (**7**)

A solution of 0.0426 g (2.5 × 10^{-4} mol) of CuCl₂·2H₂O and 0.1267 g (5 × 10^{-4} mol) of the ligand *seabz* in 15 mL of ethanol was stirred under reflux for 30 min. The solvent was evaporated under heating and the precipitate was filtered and washed with 10 mL of cold ethanol. Yield: 80%. Anal. calculated for $CuC_{22}H_{34}N_6O_6S_2Cl_2$: C, 39.11%; H, 5.08%; N, 12.45%; S, 9.47%. Experimental: C, 39.17%; H, 5.44%; N, 12.68%; S, 7.97%. IR (ν cm^{-1}): m 3397 ν_{as}(NH₂), m 3308 ν_s(NH₂), vs. 1645 ν(C=C) + δ_{sc}(NH₂) + ν(C2-N3), s 1558 ν(C=N) + ρ(NH₂) + ν(C2-N10), s 1294 ν_{as}(SO₂), s 1125 ν_s(SO₂).

3.3.8. [Cu(seabz)₂Br₂] (**8**)

A solution of 0.0558 g (2.5 × 10^{-4} mol) of CuBr₂ and 0.1267 g (5 × 10^{-4} mol) of the ligand in 15 mL of ethanol was stirred under reflux for 30 min. The solution of the reaction mixture was evaporated under heating. The precipitate was filtered and washed with 10 mL of cold ethanol. Yield: 81%. Anal. calculated for $CuC_{22}H_{30}N_6O_4S_2Br_2$: C, 36.20%; H, 4.14%; N, 11.51%; S, 8.79%. Experimental: C, 36.40%; H, 4.46%; N, 11.66%; S, 8.18%. IR (ν cm^{-1}): m 3388 ν_{as}(NH₂), m 3321 ν_s(NH₂), vs. 1639 ν(C=C) + δ_{sc}(NH₂) + ν(C2-N3), s 1549 ν(C=N) + ρ(NH₂) + ν(C2-N10), s 1289 ν_{as}(SO₂), s 1123 ν_s(SO₂).

3.3.9. [Zn(sfabz)₂Cl₂] (**9**)

A solution of the ligand (0.1507 g, 0.5 mmol) and ZnCl₂ (0.0341 g, 0.25 mmol) in 15 mL of ethanol was stirred under reflux for 30 min. The reaction mixture was left to stand at room temperature. The obtained product was filtered and washed with 10 mL of cold ethanol. The compound was dissolved in acetone. Crystals suitable for X-ray diffraction were obtained by slow evaporation of the solvent. Yield: 84%. Anal. calculated for $ZnC_{30}H_{31}N_6O_{4.5}S_2Cl_2$: C, 48.17%; H, 4.18%; N, 11.23%; S, 8.57%. Experimental: C, 48.17%; H, 3.35%; N, 11.28%; S, 8.39%. IR (ν cm^{-1}): m 3390 ν_{as}(NH₂), m 3315 ν_s(NH₂), vs. 1646 ν(C=C) + δ_{sc}(NH₂) + ν(C2-N3), vs. 1556 ν(C=N) + ρ(NH₂) + ν(C2-N10), s 1293 ν_{as}(SO₂), s 1142 ν_s(SO₂).

3.3.10. [Zn(sfabz)₂Br₂] (**10**)

A mixture of the ligand (0.1507 g, 0.5 mmol) and ZnBr₂ (0.0563 g, 0.25 mmol) in 15 mL of ethanol was stirred under reflux for 30 min. The reaction mixture was left to stand at room temperature. The reaction mixture was left to stand at room temperature. The obtained product was filtered and washed with 10 mL of cold ethanol. The compound

was dissolved in acetone. Crystals suitable for X-ray diffraction were obtained by slow evaporation of the solvent. Yield: 78%. Anal. calculated for $ZnC_{30}H_{30}N_6O_4S_2Br_2$: C, 43.52%; H, 3.65%; N, 10.15%; S, 7.28%. Experimental: C, 43.28%; H, 3.30%; N, 10.11%; S, 7.28 IR (ν cm^{-1}): m 3415 $\nu_{as}(NH_2)$, m 3312 $\nu_s(NH_2)$, s 1627 $\nu(C=C) + \delta_{sc}(NH_2) + \nu(C2\text{-}N3)$, vs. 1552 $\nu(C=N) + \rho(NH_2) + \nu(C2\text{-}N10)$, vs. 1290 $\nu_{as}(SO_2)$, vs. 1136 $\nu_s(SO_2)$.

3.3.11. [Zn(seabz)$_2$Cl$_2$] (11)

A solution of the ligand (0.1267 g, 0.5 mmol) and $ZnCl_2$ (0.0341 g, 0.25 mmol) in 15 mL of ethanol was stirred under reflux for 30 min. The reaction mixture was left to stand at room temperature. The obtained product was filtered and washed with 10 mL of cold ethanol. The reaction mixture was left to stand at room temperature. The obtained product was filtered and washed with 10 mL of cold ethanol. The compound was dissolved in acetonitrile. Crystals suitable for X-ray diffraction were obtained by slow evaporation of the solvent. Yield: 79%. Anal. calculated for $ZnC_{22}H_{32}N_6O_5S_2Cl_2$: C, 39.98%; H, 4.88%; N, 12.72%; S, 9.70%. Experimental: C, 40.02%; H, 5.46%; N, 13.12%; S, 9.08%. IR (ν cm^{-1}): m 3411 $\nu_{as}(NH_2)$, m 3328 $\nu_s(NH_2)$, vs. 1650 $\nu(C=C) + \delta_{sc}(NH_2) + \nu(C2\text{-}N3)$, s 1562 $\nu(C=N) + \rho(NH_2) + \nu(C2\text{-}N10)$, s 1295 $\nu_{as}(SO_2)$, s 1128 $\nu_s(SO_2)$.

3.3.12. [Zn(seabz)$_2$Br$_2$] (12)

A solution of the ligand (0.1267 g, 0.5 mmol) and $ZnBr_2$ (0.0563 g, 0.25 mmol) in 15 mL of ethanol was stirred under reflux for 30 min. The reaction mixture was left to stand at room temperature. The obtained product was filtered and washed with 10 mL of cold ethanol. Yield: 92%. Anal. calculated for $ZnC_{22}H_{30}N_6O_4S_2Br_2$: C, 36.11%; H, 4.13%; N, 11.48%; S, 8.76%. Experimental: C, 35.87%; H, 3.86%; N, 11.90%; S, 7.62%. IR (ν cm^{-1}): s 3400 $\nu_{as}(NH_2)$, m 3330 $\nu_s(NH_2)$, vs. 1640 $\nu(C=C) + \delta_{sc}(NH_2) + \nu(C2\text{-}N3)$, vs. 1550 $\nu(C=N) + \rho(NH_2) + \nu(C2\text{-}N10)$, vs. 1290 $\nu_{as}(SO_2)$, vs. 1124 $\nu_s(SO_2)$.

3.3.13. [Cd(sfabz)$_2$Cl$_2$] (13)

A solution of the ligand (0.1507 g, 0.5 mmol) and $CdCl_2·2.5H_2O$ (0.0572 g, 0.25 mmol) in 15 mL of ethanol was stirred under reflux for 30 min. The reaction mixture was left to stand at room temperature. The obtained product was filtered and washed with 10 mL of cold ethanol. Yield: 90%. Anal. calculated for $CdC_{30}H_{30}N_6O_4S_2Cl_2$: C, 45.84%; H, 3.85%; N, 10.69%; S, 8.16%. Experimental: C, 46.10%; H, 3.88%; N, 10.82%; S, 7.21%. IR (ν cm^{-1}): m 3419 $\nu_{as}(NH_2)$, s 3356 $\nu_s(NH_2)$, vs. 1655 $\nu(C=C) + \delta_{sc}(NH_2) + \nu(C2\text{-}N3)$, s 1568 $\nu(C=N) + \rho(NH_2) + \nu(C2\text{-}N10)$, s 1289 $\nu_{as}(SO_2)$, vs. 1144 $\nu_s(SO_2)$.

3.3.14. [Cd(seabz)$_2$Cl$_2$] (14)

A solution of the ligand (0.1267 g, 0.5 mmol) and $CdCl_2·2.5H_2O$ (0.0572 g, 0.25 mmol) in 15 mL of ethanol was stirred under reflux for 30 min. The reaction mixture was left to stand at room temperature. The obtained product was filtered and washed with 10 mL of cold ethanol. The compound was dissolved in acetonitrile. Crystals suitable for X-ray diffraction were obtained by slow evaporation of the solvent. Yield: 89%. Anal. calculated for $CdC_{22}H_{31}N_6O_{4.5}S_2Cl_2$: C, 37.80%; H, 4.47%; N, 12.02%; S, 9.18%. Experimental: C, 37.96%; H, 4.77%; N, 11.73%; S, 8.13%. IR (ν cm^{-1}): m 3400 $\nu_{as}(NH_2)$, s 3332 $\nu_s(NH_2)$, vs. 1648 $\nu(C=C) + \delta_{sc}(NH_2) + \nu(C2\text{-}N3)$, vs. 1558 $\nu(C=N) + \rho(NH_2) + \nu(C2\text{-}N10)$, vs. 1295 $\nu_{as}(SO_2)$, s 1127 $\nu_s(SO_2)$.

3.3.15. [Hg(sfabz)$_2$Cl$_2$] (15)

A solution of the ligand (0.1507 g, 0.5 mmol) and $HgCl_2$ (0.0679 g, 0.25 mmol) in 15 mL of ethanol was stirred under reflux for 30 min. The reaction mixture was left to stand at room temperature. The obtained product was filtered and washed with 10 mL of cold ethanol. Yield: 93%. Anal. calculated for $HgC_{30}H_{30}N_6O_4S_2Cl_2$: C, 41.22%; H, 3.46%; N, 9.61%; S, 7.34%. Experimental: C, 41.10%; H, 3.35%; N, 9.91%; S, 6.40%. IR

(ν cm^{-1}): m 3387 ν_{as}(NH$_2$), s 3311 ν_s(NH$_2$), vs. 1645 ν(C=C) + δ_{sc}(NH$_2$) + ν(C2-N3), s 1552 ν(C=N) + ρ(NH$_2$) + ν(C2-N10), vs. 1292 ν_{as}(SO$_2$), vs. 1141 ν_s(SO$_2$).

3.3.16. [Hg(seabz)$_2$Cl$_2$] (16)

A solution of the ligand (0.1267 g, 0.5 mmol) and HgCl$_2$ (0.0678 g, 0.25 mmol) in 15 mL of ethanol was stirred under reflux for 30 min. The reaction mixture was left to stand at room temperature. The obtained product was filtered and washed with 10 mL of cold ethanol. The compound was dissolved in acetonitrile. Crystals suitable for X-ray diffraction were obtained by slow evaporation of the solvent. Yield: 68%. Anal. calculated for HgC$_{22}$H$_{30}$N$_6$O$_4$S$_2$Cl$_2$: C, 33.96%; H, 3.89%; N, 10.80%; S, 8.24%. Experimental: C, 33.95%; H, 4.28%; N, 10.73%; S, 7.08%. IR (ν cm^{-1}): m 3403 ν_{as}(NH$_2$), m 3331 ν_s(NH$_2$), vs. 1647 ν(C=C) + δ_{sc}(NH$_2$) + ν(C2-N3), s 1559 ν(C=N) + ρ(NH$_2$) + ν(C2-N10), s 1295 ν_{as}(SO$_2$), s 1125 ν_s(SO$_2$).

3.4. Physical Measurements

FT IR spectra were recorded with an FT-IR/FT-FIR Spectrum 400 spectrophotometer using a universal ATR accessory Perkin-Elmer (4000–400 cm^{-1}). Selected vibrations and their intensities are presented in Table S1. The UV-Vis-NIR spectra (diffuse reflectance, 40,000–5000 cm^{-1}) were recorded on a Cary-5000 (Varian) spectrophotometer, spectra recorded in solution for the copper(II) compounds was obtained from a 1×10^{-3} M solution of the compounds in DMSO. Elemental analyses were conducted in a Fisons EA 1180 analyzer. The ^{1}H and ^{13}C NMR spectra were recorded with a Varian Unity Inova spectrometer with a frequency of 400 MHz for ^{1}H and 100 MHz for ^{13}C, using DMSO-d^6 as solvent, chemical shifts (δ) are reported in ppm referred to tetramethylsilane (TMS).

3.5. Solution Studies

In order to study the stability of the copper(II) compounds in solution, their spectra were recorded in DMSO (1×10^{-3}M) on a Cary-5000 (Varian) spectrophotometer for 24 h. For the zinc(II) compounds, their 1H-NMR spectra were obtained using a Varian Unity Inova spectrometer with a frequency of 400 MHz, using DMSO-d6 as solvent, chemical shifts (δ) are reported in ppm referred to tetramethylsilane (TMS).

3.6. X-ray Crystallography

X-ray diffraction data for the ligands and the compounds **1**, **2**, **3** and **10** were obtained using standard procedures on an Oxford Diffraction Gemini "A" instrument with a CCD area detector using graphite-monochromated Mo(Kα) radiation for both ligands and the compounds **1**, **2** and **3**, and Cu(Kα) for compound **10**. Data for both ligands and the compounds **1**, **2**, **3** and **10** were obtained at 130 K. Intensities were measured using $\varphi + \omega$ scans.

Diffraction data for compounds **5** and **9** were obtained on a Bruker D8 Venture\k-geometry diffractometer equipped with a CCD detector using graphite-monochromated Mo(Kα) radiation at 293.15 K for compound **5**, and 150 K for compound **9**. All structures were solved using direct methods, using the package SHELXS-2012 and refined with an anisotropic approach for non-hydrogen atoms using the SHELXL-2014/7 program. All hydrogen atoms that couldn't be detected were positioned geometrically as riding on their parent atoms, with C–H = 0.93–0.99 A and Uiso(H) = −1.2Ueq(C) for aromatic and methylene groups [53–55]. All crystallographic data can be found in Tables S2–S4.

3.7. Cell Growth Inhibition

3.7.1. Cell Culture

HeLa (cervix-uterine) MCF-7 (breast), HCT-15 (colorectal) and A549 (lung) human carcinoma cell lines, and L929 mouse fibroblast, were acquired from ATCC (American Tissue Culture Collection) and maintained in incubation at 310 K and 5% CO$_2$ with RPMI (GIBCO$^®$, Invitrogen corporation) supplemented with 10% BFS (GIBCO$^®$, Invitrogen cor-

poration), 1% L-glutamine and 1% penicillin/streptomycin. Experiments were performed with cells within at least 5 passages from each other. All cells were split when around 80–95% confluence was reached using 0.25% trypsin/EDTA.

3.7.2. In Vitro Growth Inhibition Assay

After plating 2×10^4 cells/well in a 96-well microplate (Costar®) with 300 μL capacity and allowed to attach incubating at 310 K for 48 h, HeLa (cervix-uterine) MCF-7 (breast), HCT-15 (colorectal) and A549 (lung) human carcinoma cell lines, and L929 mouse fibroblast were treated with *sfabz*, *seabz* and their Cu(II), and Zn(II) coordination compounds. The test metal compounds were made up in 5% DMSO and saline to give a 1 mM stock solution by initial dissolution in DMSO followed by dilution with saline. Sonication was sometimes used to facilitate complete dissolution. Serial dilutions were carried out to give final screening concentrations of ligands and the coordination compounds of 400, 200, and 20 μM (final concentration of DMSO of 0.5% (v/v)). Aliquots of 50 μL of these solutions were added to the wells (in triplicate) already containing 150 μL of media, so that the final concentrations were 100, 50 and 5 μM (final concentration of DMSO of 0.125% (v/v)). The cells were exposed to the complex for 24 h, which then was removed and the cells washed with washing media followed by the addition of 200 μL of fresh RPMI media. Then the cells were incubated for 72 h of recovery time. The remaining biomass was then estimated by the sulforhodamine B assay [56] (SRBassay). The three screening concentrations were used in an initial test of activity. The selected complexes were then tested for half maximal inhibitory concentration (IC$_{50}$) value determination. The previously described assay was then repeated but using six different concentrations of complex instead, ranging from 0.1 to 100 μM. Each assay was performed in triplicate. IC$_{50}$ values were obtained from plots of % cell survival against log of the drug concentration.

4. Conclusions

Novel sulfone ethyl and phenyl 2-aminobenzimidazole derivatives were designed and synthesized, based on our previous work investigating the relevance of the substituents in heterocyclic ligands in terms of their structural and biological properties. The amino group participated in intramolecular hydrogen bonding, giving rise to dimeric and tetrameric arrangements of the ligands. Interestingly, the ethyl and phenyl substitution in the alkyl sulfonated chain modified the nature of the non-covalent interactions; *seabz* depicted a lp···π_{bz} while *sfabz* showed a H···π_{phe}. In their coordination compounds, a tetrahedral geometry was stabilized for all metal ions.

For *seafz*, most of the coordination compounds presented great disorder in the substituted terminal chain, as a consequence, no suitable crystals for X-ray diffraction were obtained and only their molecular connectivity was analyzed. On the other hand, the phenyl substituent of *sfabz* gave rise to different interactions, allowing the crystallization of compounds with different transition metal ions. In the coordination compounds with *sfabz*, the presence of the terminal phenyl group induced intramolecular H···π interactions, as well as intermolecular π···π stacking and hydrogen bonding between the NH$_2$ and the sulfone group. Alternatively, for the nickel(II) compound **3** with *seafz*, the interactions observed were mainly lp···π, both intra and intermolecular.

The antiproliferative activity of all compounds was investigated resulting in two copper(II) *sfabz* derivatives showing good selectivity towards the HeLa cell line, and thus are worthy of further investigation.

Supplementary Materials: The following supporting information can be downloaded at: https://www.mdpi.com/article/10.3390/inorganics11100392/s1, Table S1. Representative vibrations and intensities for the ligands sfabz and seabz, seabz and their coordination compounds; Table S2. Crystallographic data of *sfabz*, *seabz* and compound 1.; Table S3. Crystallographic data of 2, 3 and 5.; Table S4. Crystallographic data of 9 and 10.; Table S5. ^{1}H-NMR for *sfabz* and its coordination compounds (DMSO d^6).; Table S6. ^{13}C-NMR for *sfabz* and its coordination compounds (DMSO d^6).; Table S7. ^{1}H-NMR for *seabz* and its coordination compounds (d^6 DMSO).; Table S8. ^{13}C-NMR for *seabz* and

its coordination compounds (d^6 DMSO). Figure S1. IR spectrum of sfabz; Figure S2. IR spectrum of seabz; Figure S3. IR spectrum of [Hg(sfabz)$_2$Cl$_2$]; Figure S4. IR spectrum of [Ni(seabz)$_2$Cl$_2$]; Figure S5. Solution spectrum of [Cu(sfabz)$_2$Cl$_2$] in DMSO, 1×10^{-3} M.; Figure S6. Diffuse reflectance spectrum of [Cu(sfabz)$_2$Cl$_2$].

References

1. Alderden, R.A.; Hall, M.D.; Hambley, T.W. The Discovery and Development of Cisplatin. *J. Chem. Educ.* **2006**, *83*, 728–734. [CrossRef]
2. Wang, Y.; Wang, X.; Wang, J.; Zhao, Y.; He, W.; Guo, Z. Noncovalent Interactions between a Trinuclear Monofunctional Platinum Complex and Human Serum Albumin. *Inorg. Chem.* **2011**, *50*, 12661–12668. [CrossRef]
3. Qu, Y.; Kipping, R.G.; Farrell, N.P. Solution studies on DNA interactions of substitution-inert platinum complexes mediated via the phosphate clamp. *Dalton Trans.* **2015**, *44*, 3563–3572. [CrossRef] [PubMed]
4. Miller, R.P.; Tadagavadi, R.K.; Ramesh, G.; Reeves, W.B. Mechanisms of Cisplatin Nephrotoxicity. *Toxins* **2010**, *2*, 2490–2518. [CrossRef] [PubMed]
5. Laurell, G.; Jungnelius, U. High-dose cisplatin treatment: Hearing loss and plasma concentrations. *Laryngoscope* **1990**, *100*, 724–734. [CrossRef]
6. Bruijnincx, P.C.A.; Sadler, P.J. New trends for metal complexes with anticancer activity. *Curr. Opin. Chem. Biol.* **2008**, *12*, 197–206. [CrossRef]
7. Hernández-Romero, D.; Rosete-Luna, S.; López-Monteon, A.; Chávez-Piña, A.; Pérez-Hernández, N.; Marroquín-Flores, J.; Cruz-Navarro, A.; Pesado-Gómez, G.; Morales-Morales, D.; Colorado-Peralta, R. First-row transition metal compounds containing benzimidazole ligands: An overview of their anticancer and antitumor activity. *Coord. Chem. Rev.* **2021**, *439*, 213930–213981. [CrossRef]
8. Erxleben, A. Interactions of copper complexes with nucleic acids. *Coord. Chem. Rev.* **2018**, *360*, 92–121. [CrossRef]
9. Erxleben, A. Investigation of Non-covalent Interactions of Metal Complexes with DNA in Cell-free Systems. *Chimia* **2017**, *71*, 102–111. [CrossRef]
10. Zoroddu, M.A.; Aaseth, J.; Crisponi, G.; Medici, S.; Peana, M.; Nurchi, V.M. The essential metals for humans: A brief overview. *J. Inorg. Biochem.* **2019**, *195*, 120–129. [CrossRef]
11. Pages, B.J.; Ang, D.L.; Wright, E.P.; Aldrich-Wright, J.R. Metal complex interactions with DNA. *Dalton Trans.* **2015**, *44*, 3505–3526. [CrossRef] [PubMed]
12. Zhou, P.; Huang, J.; Tian, F. Specific noncovalent interactions at protein-ligand interface: Implications for rational drug design. *Curr. Med. Chem.* **2012**, *19*, 226–238. [CrossRef] [PubMed]
13. Lu, J.P.; Yuan, X.H.; Yuan, H.; Wang, W.L.; Wan, B.; Franzblau, S.G.; Ye, Q.Z. Inhibition of Mycobacterium tuberculosis methionine aminopeptidases by bengamide derivatives. *Chem. Med. Chem.* **2011**, *6*, 1041–1048. [CrossRef]
14. Lu, J.P.; Yuan, X.H.; Ye, Q.Z. Structural analysis of inhibition of Mycobacterium tuberculosis methionine aminopeptidase by bengamide derivatives. *Eur. J. Med. Chem.* **2012**, *47*, 479–484. [CrossRef]
15. Rehman, S.U.; Sarwar, T.; Husain, M.A.; Ishqi, H.M.; Tabish, M. Studying non-covalent drug-DNA interactions. *Arch. Biochem. Biophys.* **2015**, *576*, 49–60. [CrossRef]
16. Burge, S.; Parkinson, G.N.; Hazel, P.; Todd, A.K.; Neidle, S. Quadruplex DNA: Sequence, topology and structure. *Nucleic Acids Res.* **2006**, *34*, 5402–5415. [CrossRef]
17. Reed, J.E.; Arnal, A.A.; Neidle, S.; Vilar, R. Stabilization of G-Quadruplex DNA and Inhibition of Telomerase Activity by Square-Planar Nickel(II) Complexes. *J. Am. Chem. Soc.* **2006**, *128*, 5992–5993. [CrossRef] [PubMed]

18. Sabater, L.; Fang, P.J.; Chang, C.F.; De Rache, A.; Prado, E.; Dejeu, J.; Garofalo, A.; Lin, J.H.; Mergny, J.L.; Defrancq, E.; et al. Cobalt(iii)porphyrin to target G-quadruplex DNA. *Dalton Trans.* **2015**, *44*, 3701–3707. [CrossRef] [PubMed]

19. Stafford, V.S.; Suntharalingam, K.; Shivalingam, A.; White, A.J.P.; Mann, D.J.; Vilar, R. Syntheses of polypyridyl metal complexes and studies of their interaction with quadruplex DNA. *Dalton Trans.* **2015**, *44*, 3686–3700. [CrossRef]

20. Gratteri, P.; Massari, L.; Michelucci, E.; Rigo, R.; Messori, L.; Cinellu, M.A.; Musetti, C.; Sissi, C.; Bazzicalupi, C. Interactions of selected gold(III) complexes with DNA G quadruplexes. *Dalton Trans.* **2015**, *44*, 3633–3639. [CrossRef]

21. Malina, J.; Farrell, N.P.; Brabec, V. DNA Condensing Effects and Sequence Selectivity of DNA Binding of Antitumor Noncovalent Polynuclear Platinum Complexes. *Inorg. Chem.* **2014**, *53*, 1662–1671. [CrossRef] [PubMed]

22. Navarro-Peñaloza, R.; Landeros-Rivera, B.; López-Sandoval, H.; Castro-Ramírez, R.; Barba-Behrens, N. New insights on transition metal coordination compounds with biological active azole and nitroimidazole derivatives. *Coord. Chem. Rev.* **2023**, *494*, 215360. [CrossRef]

23. Alfaro-Fuentes, I.; Castro-Ramírez, R.; Ortiz-Pastrana, N.; Medina-Guerrero, R.M.; Soler-Jiménez, L.C.; Martínez-Rodríguez, I.; Bethancourt-Lozano, M.; Ibarra-Castro, L.; Barba-Behrens, N.; Fajer-Ávila, E.J. Novel antihelmintic activity of tinidazole coordination compounds. Relevance of the metal ion and structural properties. *J. Inorg. Biochem.* **2017**, *176*, 159–167. [CrossRef]

24. Santra, R.C.; Sengupta, K.; Dey, R.; Shireen, T.; Das, O.; Duin, P.S.; Mukhopashyay, K.; Das, S. X-ray crystal structure of a Cu(II) complex with the antiparasitic drug tinidazole, interaction with calf thymus DNA and evidence for antibacterial activity. *J. Coord. Chem.* **2014**, *67*, 265–285. [CrossRef]

25. Nandy, P.; Santra, R.C.; Lahiri, D.; Nag, M.; Das, S. In Situ Reactivity of Electrochemically Generated Nitro Radical Anion on Tinidazole and Its Monomeric and Dimeric Cu^II Complexes on Model Biological Targets with Relative Manifestation of Preventing Bacterial Biofilm Formation. *ACS Omega* **2022**, *7*, 8268–8280. [CrossRef] [PubMed]

26. Castro-Ramírez, R.; Ortiz-Pastrana, N.; Caballero, A.B.; Zimmermann, M.T.; Stadelman, B.S.; Gaertner, A.A.E.; Brumaghim, J.L.; Korrodi-Gregório, L.; Pérez-Tomás, R.; Gamez, P.; et al. DNA interactions of non-chelating tinidazole-based coordination compounds and their structural, redox and cytotoxic properties. *Dalton Trans.* **2018**, *47*, 7551–7560. [CrossRef]

27. Ramírez-Palma, L.G.; Castro-Ramírez, R.; Lozano-Ramos, L.; Galindo-Murillo, R.; Barba-Behrens, N.; Cortés-Guzmán, F. DNA recognition site of anticancer tinidazole copper(ii) complexes. *Dalton Trans.* **2023**, *52*, 2087–2095. [CrossRef]

28. Novoa-Ramírez, C.S.; Silva-Becerril, A.; González-Ballesteros, M.M.; Flores-, M.; Ortiz-Frade, L.; Gracia-Mora, J.; Ruiz-Azuara, L. Biological activity of mixed chelate copper(II) complexes, with substituted diimine and tridentate Schiff bases (NNO) and their hydrogenated derivatives as secondary ligands: Casiopeína's fourth generation. *J. Inorg. Biochem.* **2023**, *242*, 112097. [CrossRef]

29. Pessoa, J.C.; Correia, I. Salan vs. salen metal complexes in catalysis and medicinal applications: Virtues and pitfalls. *Coord. Chem. Rev.* **2019**, *388*, 227–247. [CrossRef]

30. Hangan, A.C.; Lucaciu, R.L.; Turza, A.; Dican, L.; Sevastre, B.; Páll, E.; Oprean, L.S.; Borodi, G. New Copper Complexes with Antibacterial and Cytotoxic Activity. *Int. J. Mol. Sci.* **2023**, *24*, 13819. [CrossRef]

31. Alem, M.B.; Damena, T.; Desalegn, T.; Koobotse, M.; Eswaramoorthy, R.; Ngwira, K.J.; Ombito, J.O.; Zachariah, M.; Demissie, T.B. Cytotoxic mixed-ligand complexes of Cu(II): A combined experimental and computational study. *Front. Chem.* **2022**, *10*, 1028957. [CrossRef] [PubMed]

32. Ali, A.; Banerjee, S.; Kamaal, S.; Usman, M.; Das, N.; Afzal, M.; Alarifi, A.; Sepay, N.; Roy, P.; Ahmad, M. Ligand substituent effect on the cytotoxicity activity of two new copper(II) complexes bearing 8-hydroxyquinoline derivatives: Validated by MTT assay and apoptosis in MCF-7 cancer cell line (human breast cancer). *RSC Adv.* **2021**, *11*, 14362. [CrossRef] [PubMed]

33. Karges, J.; Xiong, K.; Blacque, O.; Chao, H.; Gasser, G. Highly cytotoxic copper(II) terpyridine complexes as anticancer drug candidates. *Inorg. Chim. Acta* **2021**, *516*, 120137. [CrossRef]

34. Enslin, L.E.; Purkait, K.; Pozza, M.D.; Saubamea, B.; Mesdom, P.; Gasser, G.; Schutte-Smith, M. Unique Metal-Ligand Interplay in Directing Discrete and Polymeric Derivatives of Isomeric Azole-Carboxylate. Varying Electronic Form, C-C Coupling, and Receptor Feature. *Inorg. Chem.* **2023**, *62*, 7779–7794. [CrossRef]

35. da Silva dos Reis Conde, C.A.; Querino, A.L.A.; Silva, H.; Navarro, M. Silver(I) complexes containing N-heterocyclic carbene azole drugs: Synthesis, characterization, cytotoxic activity, and their BSA interactions. *J. Inorg. Biochem.* **2023**, *246*, 112303. [CrossRef]

36. Navarro, M.; Higuera-Padilla, A.R.; Arsenak, M.; Taylor, P. Synthesis, characterization, DNA interaction studies and anticancer activity of platinum–clotrimazole complexes. *Transit. Met. Chem.* **2009**, *34*, 869–875. [CrossRef]

37. Fernández-Pampín, N.; Vaquero, M.; Gil, T.; Espino, G.; Fernández, D.; García, B.; Busto, N. A [Pt(cis-1,3-diaminocycloalkane)Cl₂] analog exhibits hallmarks typical of immunogenic cell death inducers in model cancer cells. *J. Inorg. Biochem.* **2022**, *226*, 11166.

38. Navarro, M.; Justo, R.M.S.; Delgado, G.Y.S.; Visbal, G. Metallodrugs for the Treatment of Trypanosomatid Diseases: Recent Advances and New Insights. *Curr. Pharm. Des.* **2021**, *27*, 1763–1789. [CrossRef]

39. Mohamed, H.A.; Shepherd, S.; William, N.; Blundell, H.A.; Das, M.; Pask, C.M.; Lake, B.R.M.; Phillips, R.M.; Nelson, A.; Willans, C.E. Silver(I) N-Heterocyclic Carbene Complexes Derived from Clotrimazole: Antiproliferative Activity and Interaction with an Artificial Membrane-Based Biosensor. *Organometallics* **2020**, *39*, 1318–1331. [CrossRef]

40. Soba, M.; Scales, G.; Casuriaga, F.; Pérez, N.; Veiga, N.; Echeverría, G.A.; Piro, O.E.; Faccio, R.; Pérez-Díaz, L.; Gasser, G.; et al. Multifunctional organometallic compounds for the treatment of Chagas disease: Re(i) tricarbonyl compounds with two different bioactive ligands. *Dalton Trans.* **2023**, *52*, 1623–1641. [CrossRef]

41. Betanzos-Lara, S.; Gómez-Ruiz, C.; Barrón-Sosa, L.R.; Gracia-Mora, I.; Flores-Álamo, M.; Barba-Behrens, N. Cytotoxic copper(II), cobalt(II), zinc(II), and nickel(II) coordination compounds of clotrimazole. *J. Inorg. Biochem.* **2012**, *114*, 82–93. [CrossRef]

42. Betanzos-Lara, S.; Chmel, N.P.; Zimmerman, M.T.; Barron-Sosa, L.R.; Salassa, L.; Rodger, A.; Brumaghim, J.; Gracia-Mora, I.; Barba-Behrens, N. Redox-active and DNA-binding coordination complexes of clotrimazole. *Dalton Trans.* **2015**, *44*, 3673–3685. [CrossRef]

43. Zhao, X.J.; Li, J.; Ding, B.; Wang, X.G.; Yang, E.C. The irreversible crystal transformation of a novel Cadmium(II) supramolecular complex containing planar tetrameric water cluster. *Inorg. Chem. Commun.* **2007**, *10*, 605–609. [CrossRef]

44. Esparza-Ruiz, A.; Peña-Hueso, A.; Mijangos, E.; Osorio-Monreal, G.; Nöth, H.; Flores-Parra, A.; Contreras, R.; Barba-Behrens, N. Cobalt(II), nickel(II) and zinc(II) coordination compounds derived from aromatic amines. *Polyhedron* **2011**, *30*, 2090–2098. [CrossRef]

45. Durán-Solares, G.; Fugarolas-Gómez, W.; Ortíz-Pastrana, N.; López-Sandoval, H.; Villaseñor-Granados, T.O.; Flores-Parra, A.; Altmann, P.J.; Barba-Behrens, N. Lone pair···π interactions on the stabilization of intra and intermolecular arrangements of coordination compounds with 2-methyl imidazole and benzimidazole derivatives. *J. Coord. Chem.* **2018**, *71*, 1953–1958. [CrossRef]

46. Sudha, S.; Karabacak, M.; Kurt, M.; Cinar, M.; Sundaraganesan, N. Molecular structure, vibrational spectroscopic, first-order hyperpolarizability and HOMO, LUMO studies of 2-aminobenzimidazole. *Spectrochim. Acta-Part A Mol. Biomol. Spectrosc.* **2011**, *84*, 184–195. [CrossRef]

47. Lever, A.B.P. Electronic Spectra of Some Transition Metal Complexes. *J. Chem. Ed.* **1968**, *45*, 711–712. [CrossRef]

48. Mugiraneza, S.; Hallas, A.M. Nuclear and magnetic spin structure of the antiferromagnetic triangular lattice compound LiCrTe$_2$ investigated by μ+SR, neutron and X-ray diffraction. *Commun. Phys.* **2022**, *5*, 1–12.

49. Lever, A.B.P. *Inorganic Electronic Spectroscopy*; Elsevier: Amsterdam, The Netherlands, 1984.

50. Navarro-Peñaloza, R.; Vázquez-Palma, A.B.; López-Sandoval, H.; Sánchez-Bartéz, F.; Gracia-Mora, I.; Barba-Behrens, N. Coordination compounds with heterocyclic ester derivatives. Structural characterization and anti-proliferative activity. *J. Inorg. Biochem.* **2021**, *219*, 111432. [CrossRef] [PubMed]

51. Kruse, H.; Mrazikova, K.; D'Ascenzo, L.; Sponer, J.; Auffinger, P. Short but Weak: The Z-DNA Lone-Pair···π Conundrum Challenges Standard Carbon Van der Waals Radii. *Angew. Chem. Int. Ed.* **2020**, *59*, 16553–16560. [CrossRef]

52. Kalra, K.; Gorle, S.; Cavallo, L.; Oliva, R.; Chawla, M. Occurrence and stability of lone pair-π and OH–π interactions between water and nucleobases in functional RNAs. *Nucleic Acids Res.* **2020**, *11*, 5825–5838. [CrossRef] [PubMed]

53. Sheldrick, G.M. A Short History of SHELX. *Acta Crystallogr. Sect. A Found. Crystallogr.* **2008**, *64*, 112. [CrossRef] [PubMed]

54. Clark, R.C.; Reid, J.S. The analytical calculation of absorption in multifaceted crystals. *Acta Crystallogr. Sect. A Found. Crystallogr.* **1995**, *51*, 887. [CrossRef]

55. Hübschle, C.B.; Sheldrick, G.M.; Dittrich, B. ShelXle: A Qt Graphical User Interface for SHELXL. *J. Appl. Crystallogr.* **2011**, *44*, 1281–1284. [CrossRef]

56. Orellana, E.A.; Kasinski, A.L. Sulforhodamine B (SRB) Assay in Cell Culture to Investigate Cell Proliferation. *Bio-protocol* **2016**, *6*, e1984. [CrossRef]